Quantitative Precipitation Estimation and Quantitative Precipitation Forecasting by the Japan Meteorological Agency

Kazuhiko NAGATA
Forecast Division, Forecast Department
Japan Meteorological Agency

1. Introduction

Typhoons sometimes hit countries in East Asia and Southeast Asia, and may bring various hazards including sediment-related disasters, flooding and inundation. To prevent and mitigate damage from such disasters, analysis and forecasting of precipitation amounts is very important. Analysis relating to the distribution of rainfall amounts is called Quantitative Precipitation Estimation (QPE), and that relating to forecasting is called Quantitative Precipitation Forecasting (QPF). The Japan Meteorological Agency (JMA) developed QPE and QPF products as well as QPE/QPF-induced products using radar data, rain gauge data and numerical weather prediction (NWP) output. Figure 1 shows the relationships that link these various data and products, including QPE and QPF.

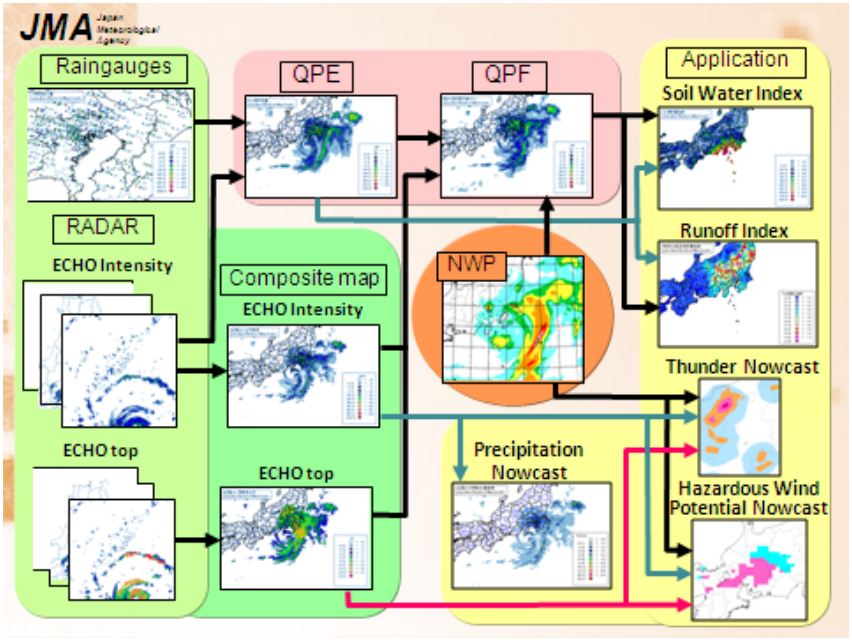

Fig. 1 Various precipitation products derived from rain gauge and radar data

2. Radar/Rain gauge-Analyzed Precipitation

Radar/Rain gauge-Analyzed Precipitation (referred to here as “R/A”) is a QPE product of JMA. It shows one-hour cumulative rainfall with a spatial resolution of 1 km, and is issued every 30 minutes. Figure 2 shows a sample.

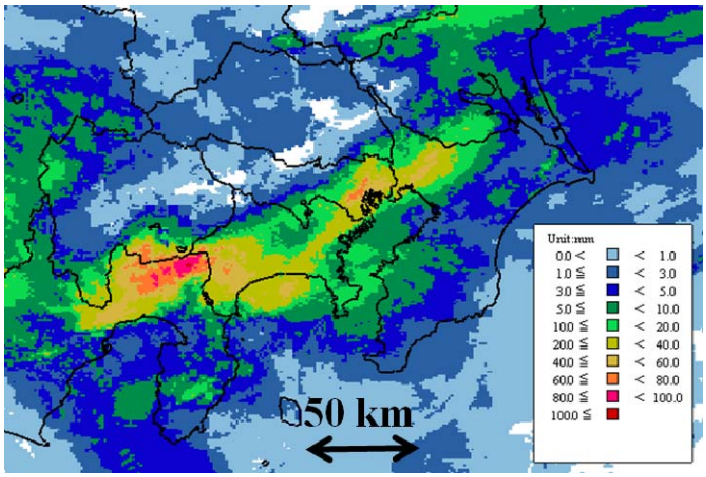

Fig. 2 Sample of R/A product (06 UTC, 8 Sep. 2010)

2.1 Observation data used to produce R/A

Both rain gauge and radar data are used to produce R/A. Although rain gauges measure precipitation amounts with satisfactory accuracy, they can observe only at a single point. Conversely, radars can observe large areas at the same time with a higher spatial resolution than the rain gauge network, but may produce readings different from those obtained with a ground-based rain gauge as they measure amounts of rain overhead. Their accuracy is also not as reliable as that of rain gauges because they are remote sensing instruments. For monitoring and prediction of sediment-related disasters, flooding and inundation, the rain gauge network is too rough and radar observation lacks sufficient accuracy. For this reason, JMA produces R/A by calibrating one-hour accumulated radar echo data with one-hour accumulated rain gauge precipitation data. It collects data from 10,000 rain gauges operated by JMA, the Ministry of Land, Infrastructure, Transport and Tourism (MLIT) and local governments every ten minutes or every hour (rain gauges are located in every 7-km grid square on average) and data from 46 C-band radars operated by JMA and MLIT with a spatial resolution of 1 km every five minutes. Each radar covers an area of 500 km × 500 km.

2.2 R/A algorithms

The procedure for producing R/A involves the following three steps:

1. Accumulation of radar intensity data
2. Calibration of radar data
3. Composition of calibrated radar data

This section briefly describes each process.

2.2.1 Accumulation of radar intensity data

First, echo intensity data obtained every five minutes are accumulated. If echoes move too fast, one-hour accumulated echo intensities sometimes show an unnatural striped pattern (see the image on the left of Fig. 3). To avoid such unnatural patterns, accumulation must be conducted taking account of echo movements (see the image on the right of Fig. 3). In this process, the observed echoes are divided into pieces and traced every five minutes. Then, by summing up the echo intensities passing a grid, the one-hour accumulated echo intensity of the grid is estimated. Quality checking of echo intensities is also conducted at this stage.

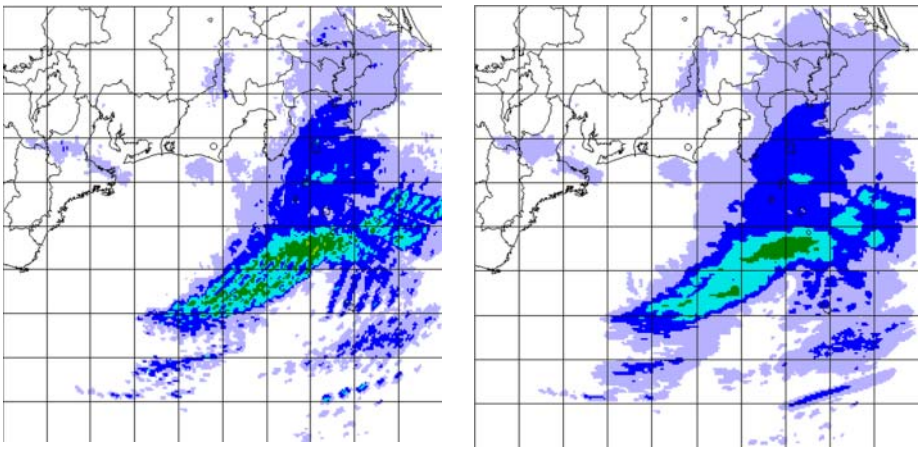

Fig. 3 Accumulation of radar intensity data
Left: one-hour accumulated echoes; right: as per the figure on the left, but with consideration of echo movements

2.2.2 Calibration of radar data

To produce accurate QPE, calibration of one-hour accumulated radar data is performed to fit the distribution of one-hour accumulated rain gauge data. Calibration is conducted in two steps. First, each piece of radar data is calibrated to fit averaged rain gauge data within the relevant observation range. Then, detailed calibration of radar data over land is conducted to fit rain gauge data on local scales.

2.2.2.1 Calibration over the whole radar observation range

Values of one-hour precipitation estimated from the accumulation of radar echo intensities in a certain grid are generally different from observation values from a rain gauge in the grid. As rain gauge measurement is more reliable, the accumulation of radar echo intensities is calibrated with rain gauge observations within the radar observation range to meet the following two conditions:

(1) The average of the calibrated accumulation for radar echo intensities over a certain domain should be equal to that of all other radars observing the same domain.
(2) The average of the calibrated accumulation for radar echo intensities over a certain grid should be equal to the average of the rain gauge observations.

Figure 4 shows a sample of this calibration. The figure on the left shows one-hour precipitation estimated

from the accumulation of radar echo intensities; the central figure shows one-hour precipitation after calibration to meet the two conditions outlined above; and the figure on the right shows the one-hour precipitation observed by rain gauges. The original accumulation of radar echo intensities (left) in a certain grid is less than the rain gauge observation in the same grid (right). Due to calibration, the central figure shows more precipitation than that on the left. The figure on the right is closer to the central figure than the left figure.

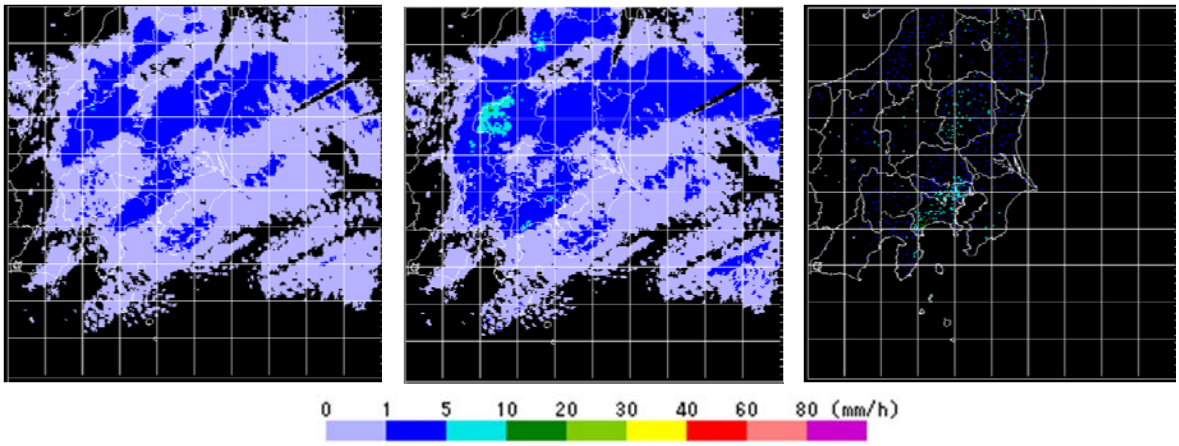

Fig. 4 Left: sample of one-hour precipitation estimated by accumulating echo intensities; center: after calibration; right: from raingauge observations

2.2.2.2 Calibration over land

The calibrated echo intensities explained above are further calibrated to enable expression of more detailed patterns of precipitation on local scales (Makihara, 2000). For example, the calibrated accumulation of echo intensities for a certain grid *g* derived using the method described in 2.2.2.1 is calibrated again using data from rain gauges within about 40 km of that grid. A calibration factor for grid *g* is calculated with weighted interpolation of the calibration factors of the surrounding grids that contain rain gauges within 40 km of the grid. Here, the calibration factor for the grid is defined as the ratio of rain gauge observation values to the calibrated accumulation of radar echo intensities in the grid using the method outlined in 2.2.2.1. The following factors are taken into account to calculate the weight of interpolation:

(1) Distances between grid *g* and rain gauges
(2) Differences between echo intensity for grid *g* and those for grids containing rain gauges
(3) Beam attenuation rate for precipitation
(4) Uniformity of rain gauge distribution

Multiplying the calibrated echo intensities by the calibration factor as determined above gives the estimated precipitation for grid *g*.

Figure 5 shows a sample of this calibration. The figure on the left shows calibrated accumulation of radar

echo intensities calculated using the method outlined in 2.2.2.2, and that on the right shows one-hour rain gauge data (in the same way as the image on the right of Fig. 4). The figure on the left matches the rain gauge data better than the central image in Fig. 4.

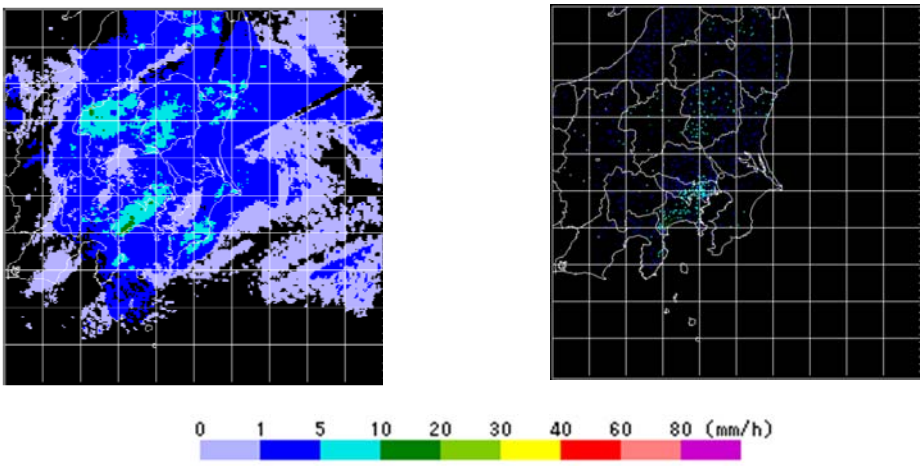

Fig. 5 Left: sample of one-hour precipitation after calibration over land; right: the corresponding raingauge observations (as per the image on the right of Fig. 4)

2.2.3 Composition of calibrated radar data

After the above calibration, a composite precipitation map is produced using the calibrated accumulation of echo intensities calculated using the method outlined in 2.2.2.2 from 46 radars located around the country by transforming the coordination from zenithal projection into latitude-longitude grids with equidistant cylindrical projection. If two or more radars observe the same grid, the greater value is selected. Figure 6 shows calibrated echo intensities covering each region and a composite precipitation map of the country.

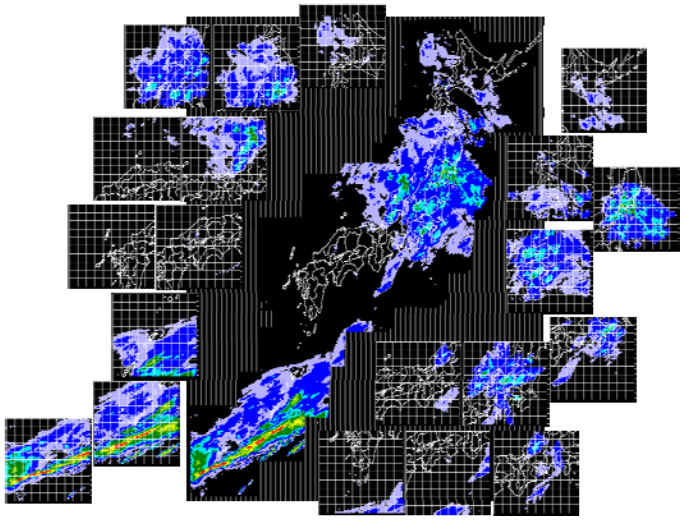

Fig. 6 Radar data covering each region and a composite precipitation map

2.3 Accuracy of R/A

To assess the accuracy of R/A, experimental R/A data for verification excluding rain gauge data at about 200 observing points were prepared, and were compared with the excluded rain gauge data. Rain gauge observation values were compared with R/A values for nine grids (a central grid and the eight grids surrounding it) considering location errors equivalent to the dimensions of one grid (i.e., 1 km) stemming from wind-related advection of raindrops before their arrival at ground level, and/or errors resulting from coordinate transform.

Figure 7 shows a scatter plot comparing hourly R/A values and corresponding rain gauge measurements taken over a period of four months during the warm season (from August to November of 2009). Only the best R/A values out of the nine grids are plotted. The figure shows close agreement between R/A values and rain gauge measurements.

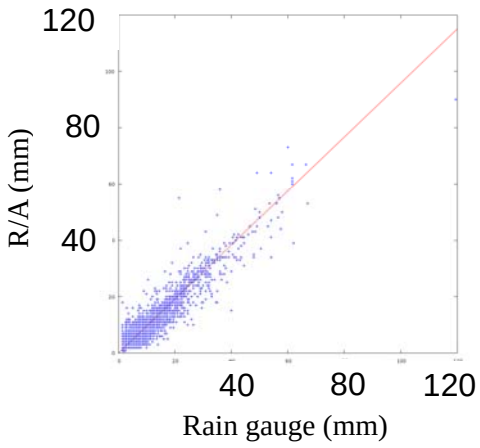

Fig. 7 Scatter plot of R/A and rain gauge data with a regression line (red) (R/A = 0.96 × Raingauge)

3. Very-short-range Forecasting of Precipitation

Very-short-range Forecasting of Precipitation (referred to here as “VSRF”) is a QPF product of JMA. It provides hourly precipitation forecasting up to six hours ahead with a spatial resolution of 1 km. VSRF is calculated by merging the forecast precipitation with values from JMA’s mesoscale model (MSM) and the extrapolated composite echo intensity. Figure 8 shows a sample of VSRF. An outline of the procedures for producing VSRF is given below.

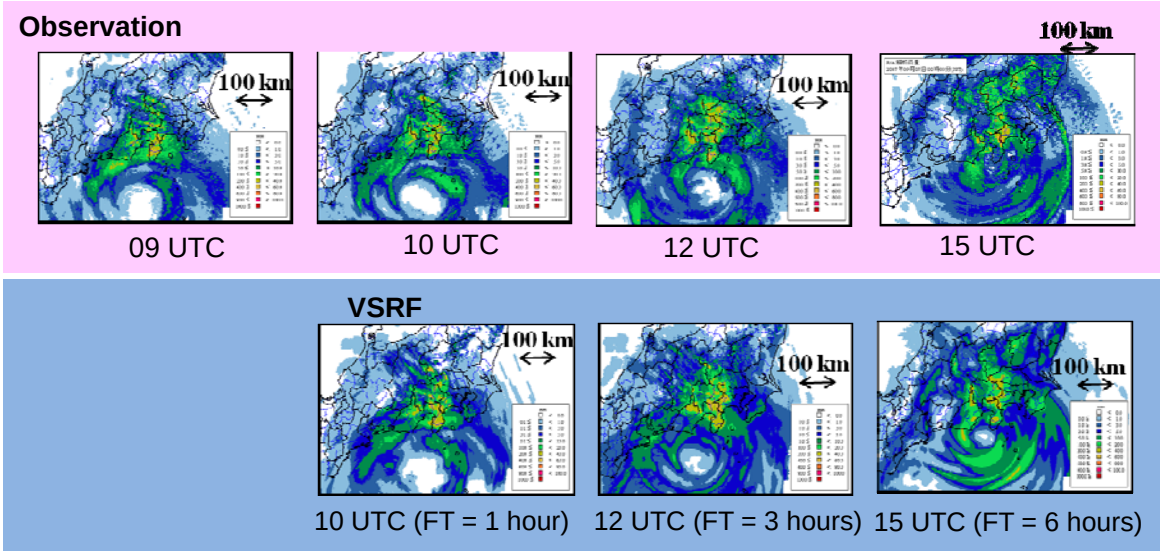

Fig. 8 Sample of VSRF (initial time: 09 UTC, 6 Sep. 2007)

3.1 VSRF algorithms

Generally, extrapolation is the best method of precipitation forecasting for a time frame within a few hours from the present. However, a numerical model gives better performance gradually over time. JMA therefore conducts VSRF by both using extrapolation and merging model output. The procedure for producing VSRF consists of two parts:

1. The extrapolation method
2. The merging method

3.1.1 Extrapolation method

3.1.1.1 Movement vectors

First, the area over Japan is divided into 50-km grid squares. Then, the movement vectors of precipitation systems are estimated for every 50-km grid using a pattern matching method, which indicates the systems' direction and speed of movement. In order to avoid any adverse influence from orographic effects on this estimation[1], time subtractions of R/A are used. Thirty candidates for movement vectors in the grid with the highest matching scores are obtained accordingly using the differences among R/A (t = 0 h), R/A (t = -1 h), R/A (t = -2) and R/A (t = -3 h). Then, the most suitable candidate vector is selected in consideration of time-space smoothness. Movement vectors gradually approach the speed of 700-hPa winds of the MSM as the forecast time increases. Figure 9 shows a sample of a movement vector (left) and the one-hour accumulated precipitation forecast with this movement vector (right).

[1] Orographic effects in a grid cause precipitation systems to look static or appear to move more slowly than they actually do.

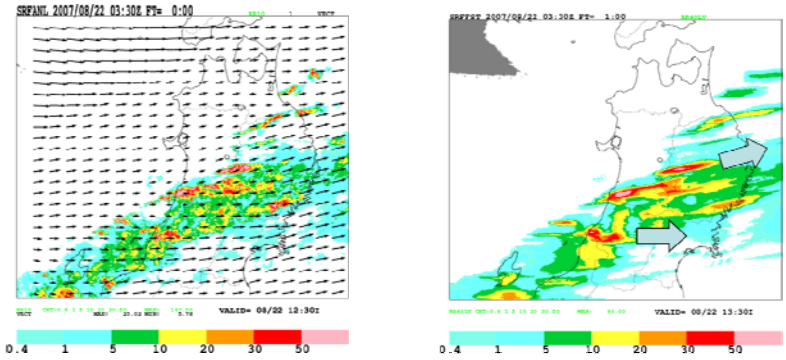

Fig. 9 Sample of movement vectors and forecast one-hour accumulated precipitation

Left: initial echo intensity (shading) and movement vectors (arrows); right: forecast one-hour accumulated precipitation. The block arrows show precipitation system direction of movement.

3.1.1.2 Orographic effects

Precipitation caused by orographic enhancement is sometimes seen to be stationary over the windward side of mountains. The algorithm follows the concept of the seeder-feeder model (Browning & Hill, 1981). Rainfall passing through a feeder cloud generated by orographic effects becomes enhanced due to water droplets in the feeder cloud.

Precipitable water, which is estimated using data for temperature, relative humidity and wind from the surface to 850 hPa in the MSM, is used to judge whether feeder clouds are generated. If so, precipitation is enhanced depending on the amount of rainfall from the seeder cloud. Figure 10 shows orographic enhancement of precipitation.

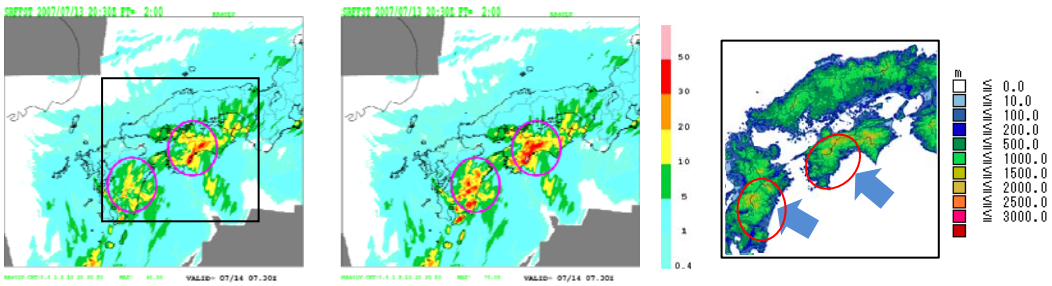

Fig. 10 Orographic enhancement (inside the circles of the figures to the left and center)

Left: forecast one-hour accumulated precipitation without orographic effects; center: as per the image on the left, but with orographic effects; right: altitude map showing the square area from the figure on the left. The block arrows show precipitation system direction of movement.

The dissipation of echo on the lee side of mountains is also considered. This occurs when the echo top is low, the angle between the directions of mid- and low-level winds is small, and no echoes are present in the dissipation area. Echo dissipation is clearer when echo intensity is stronger and the travel time from the mountaintop to the dissipation area is longer. Echo dissipation is estimated statistically from 700-hPa winds, 900-hPa winds and the relative humidity of the MSM. Figure 11 shows a case of echo dissipation.

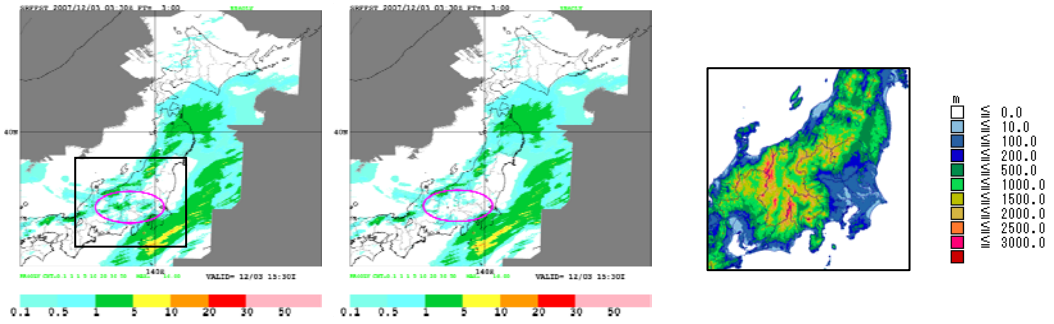

Fig. 11 Echo dissipation (inside the circles of the figures to the left and center)
Left: forecast one-hour accumulated precipitation without orographic effects; center: with orographic effects; right: topographic map with altitude showing the square areas from the figures to the left and center.

3.1.1.3 Accumulation of forecast intensity

The initial field used for VSRF is a composite echo intensity field obtained in the process of making R/A. The echo intensity field is shifted along the movement vector with a time step of two or five minutes. One-hour precipitation at a particular point is calculated as the sum of the echo intensities passing that point. In the process, enhancement and dissipation of precipitation due to orographic effects are considered.

3.1.2 Merging of extrapolation method and MSM

The performance of the conventional extrapolation method is satisfactory up to three to four hours from the initial time. For forecast times of more than six hours, the results of the MSM are considered superior to those of the extrapolation method. It is expected that four- to six-hour forecasts can be improved by merging the results of the extrapolation method and those of the MSM with a different blending ratio over time. The blending ratio is estimated from the accuracy levels of the extrapolation method and the MSM over the past few hours (Araki, 2000). VSRF is the output of this merging process, for which a sample is shown in Figure 12. The precipitation in the red circle for VSRF is from an extrapolation method forecast, and that in the blue circle is from the MSM. R/A more closely corresponds to VSRF than to extrapolation method forecasting and the MSM due to the merging of the extrapolation method forecast and the MSM.

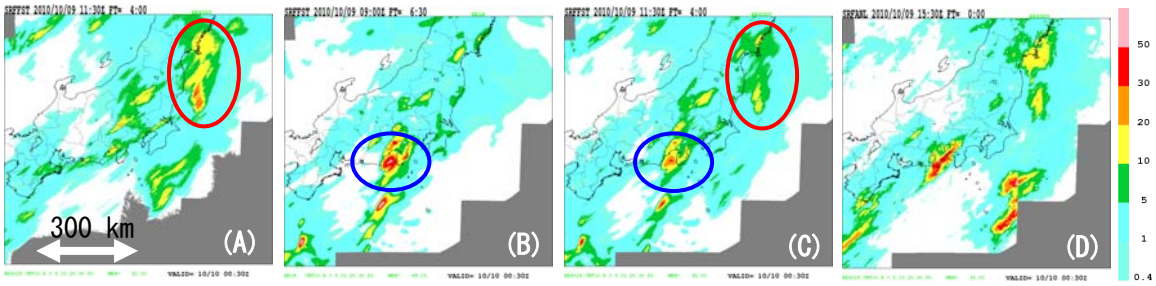

Fig. 12 Merging process

Forecasting with (A) the extrapolation method, (B) the MSM and (C) VSRF for 1530 UTC on 9 Oct., 2010, and (D) R/A for the same time. The initial time of (A) and (C) is 1130 UTC (FT = 4), and that of (B) is 0900 UTC (FT = 6.5). Precipitation in the red circle for VSRF originates from the extrapolation method, and that in the blue circle originates from the MSM. The amount of precipitation depends on the blending ratio.

3.2 Accuracy of VSRF

Critical Success Index (CSI) values for VSRF, the extrapolation method (EXT), the MSM and the persistent forecast (PST) for averaged hourly precipitation from June to August 2010 are shown in Fig. 13. Here, the region over Japan was divided into 20-km grid squares. The threshold of rainfall is 1 mm/hour. The figure shows that VSRF exhibits superior performance over the whole forecast time.

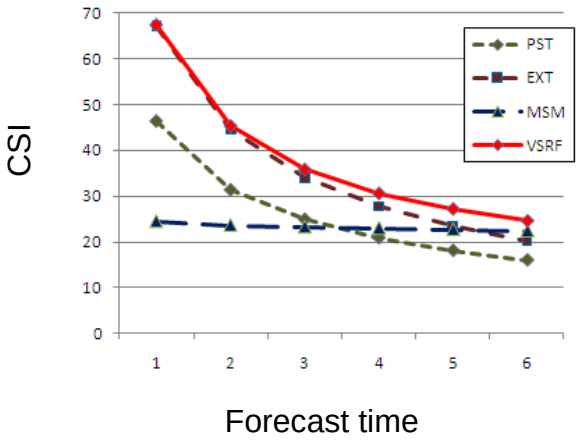

		Event observed	
		Yes	No
Event forecast	Yes	A	B
	No	C	D

$$CSI = A / (A + B + C) \times 100$$

Fig. 13 CSI of VSRF, the extrapolation method (EXT), the MSM and the persistent forecast (PST) verified from June to August 2010

4. Applications of QPE/QPF

Precipitation figures alone do not provide enough information for forecasters to monitor and forecast sediment-related disasters because such events are closely linked to the amount of moisture in the soil. JMA uses the Soil Water Index to monitor and forecast sediment-related disasters.

Precipitation figures alone also provide insufficient information for forecasters to monitor and forecast flood disasters because such events are closely linked to the amount of water outflow to rivers as well as the time lag of water as it moves along river channels. JMA uses the Runoff Index to monitor and forecast flood disasters.

4.1 Soil Water Index

The Soil Water Index (referred to here as the "SWI") is calculated up to six hours ahead with a spatial resolution of 5 km showing the risk of sediment-related disasters (debris flow, slope failure, etc.) caused by heavy rain. Figure 14 shows a sample of the SWI.

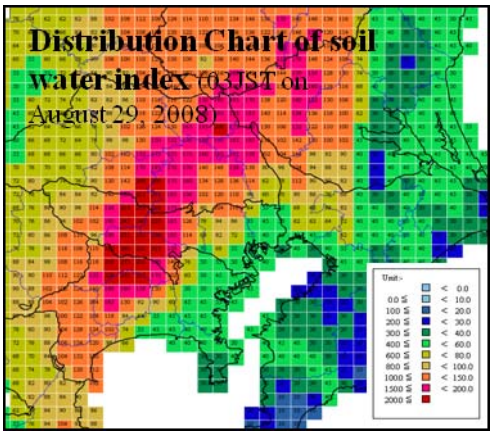

Fig. 14 Soil Water Index distribution chart

The risk of sediment-related disasters caused by heavy rain becomes higher when the amount of moisture in soil increases. Such disasters may sometimes be caused by rainfall from several days before.

The amount of moisture in the soil is indexed using the tank model method to indicate how much rainwater is contained in soil based on rainfall analysis (see Fig. 15). R/A and VSRF are used as input for the tank model.

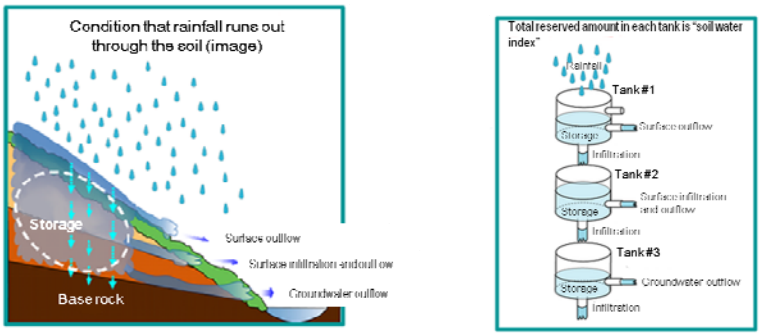

Fig. 15 Outline of tank model
Left: Condition in which rainfall runs out through soil; right: The total reserved amount in each tank is used to form the Soil Water Index.

Sediment-related disasters frequently occur in areas with high SWI values. Figure 16 shows a time-sequence representation of the SWI in a grid where a sediment-related disaster actually occurred. Its timing approximately coincided with the peak SWI value.

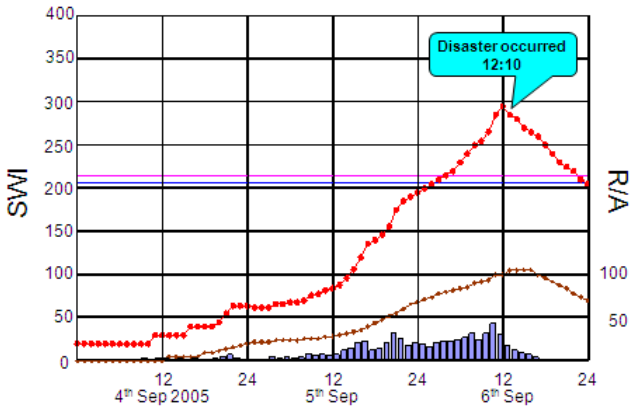

Fig. 16 Time-sequence representation of SWI and rainfall amounts in a grid where a sediment-related disaster occurred. The red line shows the SWI, the brown line shows 24-hour cumulative rainfall, and the bars show 1-hour cumulative rainfall.

Since May 2010, the SWI has been used by forecasters at JMA's meteorological observatories when issuing heavy rain warnings/advisories to call attention to the risk of sediment disasters.

4.2 Runoff Index

The Runoff Index (referred to here as the "RI") is calculated up to six hours ahead with a spatial resolution of 5 km showing the risk of flooding for individual rivers in the country. The amount of rainfall is not directly linked to the risk of flooding for the following two reasons:

1. There is a time difference between the occurrence of rainfall and increased water levels in rivers.
2. It takes time for water to run down river channels.

Accordingly, when monitoring and forecasting flood risk, the above two effects should also be carefully considered in addition to accurate QPE/QPF (see Fig. 17).

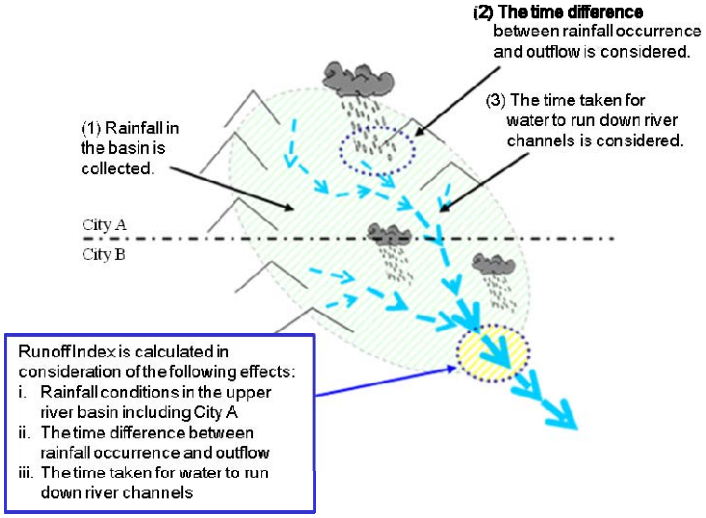

Fig. 17 Three effects to be considered in evaluating flood risk

In the RI, the tank model is used to estimate outflow, and includes the processes of water flowing down the slopes of the basin (covering an area of about 5 km × 5 km) to the river, and then down the river channel. The RI is calculated targeting rivers with a length of 15 km or more. R/A and VSRF are used as inputs for the tank model. Figure 18 shows a sample of the RI.

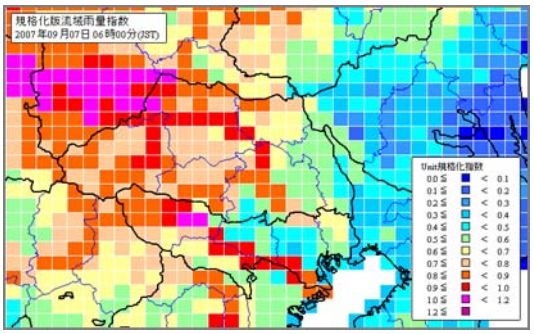

Fig. 18 Sample of the RI shown in 5-km grids

Floods frequently occur in areas with high RI values. Figure 19 shows a time series representation of the RI and water levels in a grid where actual flooding occurred. The time series corresponds closely to the water level of the river.

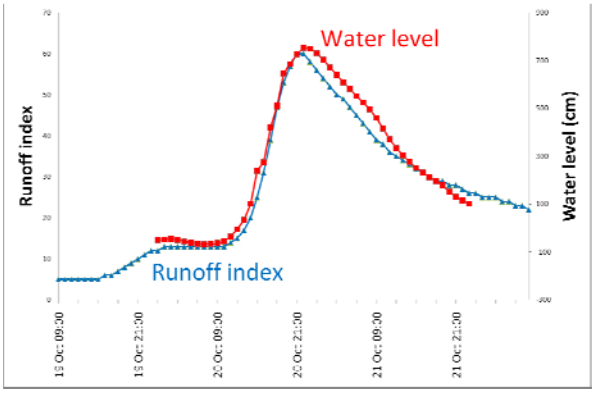

Fig. 19 Time series of the RI and water levels for a grid in which flooding occurred. The red line shows the water level, and the blue line shows the RI.

Since May 2010, the RI has been used by forecasters at JMA's meteorological observatories when issuing flood warnings/advisories to call attention to the risk of flooding.

References

Araki, K., 2000: Six-hour forecasts of precipitation. Reports of the Numerical Prediction Division, **47**, 36 – 41 (in Japanese).

Browning, K. A., F. F. Hill, 1981: Orographic Rain. Weather, **35**, 326 – 329.

Makihara, Y., 2000: Algorithms for precipitation nowcasting focused on detailed analysis using radar and raingauge data, Study on the Objective Forecasting Techniques, Technical Reports of the Meteorological Research Institute, **39**, 63 – 111.